Dynamic Holographic Gratings Recorded by Photopolymerization of Liquid Crystalline Monomers

Jian Zhang, Christopher R. Carlen, Susanna Palmer, and Michael B. Sponsler*

Contribution from the Department of Chemistry and W. M. Keck Center for Molecular Electronics, Syracuse University, Syracuse, New York 13244-4100

*Received December 13, 1993**

Abstract: Dynamic liquid crystalline gratings composed of alternating permanent and alignable regions were prepared by photopolymerization of a liquid crystalline monomer mixture with interfering laser beams from an argon ion laser (488 nm). The 6-μm-thick gratings were reversibly switched to states with modulated orientation or modulated order by application of an electric field or by heating, respectively. The structure of the gratings, with periods ranging from 10.8 to 0.35 μm, was probed through holographic diffraction of 633-nm laser light. Several diffraction orders were observed from thin-regime gratings (period = 10.8 μm), and simulation of the observed intensities indicated that the grating refractive index profiles were between sine and square wave in shape. Images of the gratings obtained through optical microscopy also provided structural information and allowed direct evaluation of spatial homogeneity. The diffraction experiments also demonstrated the potential utility of the liquid crystalline media for holographic recording, which offer clean on–off switching of diffracted light (on–off intensity ratios in the 10^2–10^3 range), minimal degradation after 10^5 switching cycles, and holographic efficiencies up to the theoretical limit for thin gratings (about 34%).

Precise control of molecular orientation and position is a necessary step for the design of molecular devices and organized assemblies. Light and external electric fields are two of the most convenient means available to achieve active control. In this report, we describe the use of these tools in the formation of dynamic holographic gratings consisting of layers of liquid crystals with modulated orientation. These gratings allow clean on–off switching of diffracted light intensity[1] and could be used as host media for control of molecular orientation over micron or submicron regions.

Holographic recording is accomplished through the preferential formation of photoproducts in the regions of constructive interference arising from the overlap of two laser beams, called object and reference beams, at a photosensitive sample (Figure 1). If the photoproducts differ from the reactants in refractive index and/or absorption, the hologram will cause diffraction of the reference beam so as to reconstruct the object wave front when the object beam is blocked before the film (the reading stage). The percentage of light energy that is diffracted in the reading stage is referred to as the diffraction or holographic efficiency. In our experiments, the reference and object beams are plane waves of equal intensity, and the resulting interference pattern is a sinusoidal grating.

Holography is a proven tool in the investigation of photochemical and photophysical processes[2] and has been applied to photopolymerization.[3] In turn, photopolymers are important recording materials for holography,[4] and some commercial films exist.[5] During the recording stage, photopolymer is formed in the regions of constructive interference, and in most of the materials, diffusion of monomer into the polymeric regions results in a density gradient that accounts for most of the refractive index modulation.

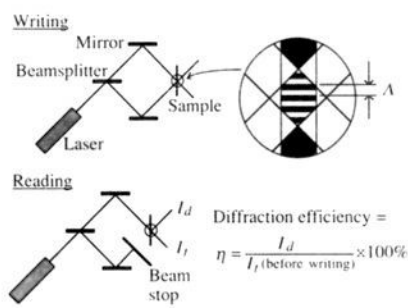

Figure 1. Writing and reading of holographic gratings. In the writing (recording) step, two laser beams of equal intensity interfere to create a sinusoidally varying intensity pattern with spacing or period of Λ. Through photochemistry, a reactant/product grating with the same spacing is formed. In the reading stage, a single beam is partially diffracted due to the modulation of refractive index and/or absorbance in the grating.

For many holographic recording media, one or more development steps are required in between the recording and reading steps in order to increase the diffraction efficiency. In addition, a fixing step may be used in order to make the hologram permanent. In some liquid crystal-containing media,[6] the diffraction efficiency can be modulated through the application of electric fields.[7] In these switchable media, the switching process represents a reversible developing step. If a fixing step is available, no switching can be done after fixing.

* Abstract published in *Advance ACS Abstracts,* June 15, 1994.

(1) (a) Zhang, J.; Sponsler, M. B. *J. Am. Chem. Soc.* **1992**, *114*, 1506–1507. (b) Zhang, J. Ph.D. Dissertation, Syracuse University, April 1993. (c) Zhang, J.; Carlen, C. R.; Palmer, S. P.; Sponsler, M. B. In *Photopolymers and Applications in Holography, Optical Data Storage, Optical Sensors, and Interconnects*; Lessard, R. A., Ed.; SPIE: Bellingham, WA, 1994; Proc. SPIE Vol. 2042, pp 238–247.

(2) (a) Bräuchle, C.; Burland, D. M. *Angew. Chem., Int. Ed. Engl.* **1983**, *22*, 582–598. (b) Eichler, H. J.; Günter, P.; Pohl, D. W. *Laser-Induced Dynamic Gratings*; Springer-Verlag: New York, 1986. (c) Odear, R. M.; Park, I. H.; Xia, K.; Johnson, C. S., Jr. *Rev. Sci. Instrum.* **1991**, *62*, 27–32. (d) Fourkas, J. T.; Fayer, M. D. *Acc. Chem. Res.* **1992**, *25*, 227–233. (e) Wang, C. H.; Xia, J. L. *J. Phys. Chem.* **1992**, *96*, 190–194.

(3) Carre, C.; Lougnot, D. J.; Fouassier, J. P. *Macromolecules* **1989**, 22, 791–799 and references cited therein.

(4) (a) Ingwall, R. T.; Troll, M. *Opt. Eng.* **1989**, *28*, 586–591. (b) Curtis, K.; Psaltis, D. *Appl. Opt.* **1992**, *31*, 7425–7428. (c) Carre, C.; Lougnot, D. J.; Renotte, Y.; Leclere, P.; Lion, Y. *J. Opt. (Paris)* **1992**, *23*, 73–79.

(5) *Holography Market Place*, 3rd ed.; Kluepfel, B., Ross, F., Eds.; Ross: Berkeley, CA, 1991; pp 30–32.

(6) Zhang, J.; Sponsler; M. B. In *Molecular and Biomolecular Electronics*; Birge, R. R., Ed.; ACS Advances in Chemistry Series No. 240; American Chemical Society: Washington, DC, Chapter 12, in press.

(7) (a) Sainov, S.; Mazakova, M.; Pantcheva, M.; Tontchev, D. *Mol. Cryst. Liq. Cryst.* **1987**, *152*, 609–615. (b) Whitney, D. H.; Ingwall, R. T. In *Photopolymer Device Physics, Chemistry, and Applications*; Lessard, R. A., Ed.; SPIE: Bellingham, WA, 1990; Proc. SPIE Vol. 1213, pp 18–26. (c) Margerum, J. D.; Lackner, A. M.; Ramos, E.; Smith, G. W.; Vaz, N. A.; Kohler, J. L.; Allison, C. R. U.S. Patent 4 938 568, 1990. Sutherland, R. L.; Natarajan, L. V.; Tondiglia, V. P.; Bunning, T. J. *Chem. Mater.* **1993**, *5*, 1533–1538. (d) Slyusar, A. V.; Myl'nikov, V. S. *Sov. Phys.—Tech. Phys.* **1991**, *36*, 1311–1312. (e) Parker, W. P. In *Practical Holography VII: Imaging and Materials*; Benton, S. A., Ed.; SPIE: Bellingham, WA, 1993; Proc. SPIE Vol. 1914, pp 176–187.

0002-7863/94/1516-7055$04.50/0

Many applications are possible for switchable holographic recording media, including switchable displays, holographic spatial light modulators, beam-steering arrays, and many other types of active optical elements. Switchable holograms represent a new class of optical components that combine the high information density of holograms with the signal modulation capability of electro-optic, acousto-optic, and spatial light modulators. Early development work on several new optical components that incorporate switchable holographic gratings has very recently been described.[8]

Although enormous advances in holographic recording have occurred since its first demonstration with lasers in 1963,[9] very few reports of recording media that allow modulation of diffraction efficiency have appeared.[6] These methods, all of which involve electric field switching of liquid crystals, use several different methods for generating the switchable holograms, including postrecording liquid crystal filling of porous[7b] or relief[7a] structures, *in-situ* formation of polymer-dispersed liquid crystals (PDLCs) through photopolymerization and phase separation of monomer/liquid crystal mixtures,[7c] and more complex procedures.[7e] Another approach involves sandwiching of liquid crystal and photoconductor layers between transparent electrodes; these media are only switchable when the writing beams are on.[7d]

In an earlier communication, we presented preliminary results on the recording of switchable holographic gratings by photopolymerization of liquid crystalline monomers, proposed to operate through a modulation of liquid crystal orientation.[1a] Our best results were obtained with the diacrylate **1**. Herein we update our

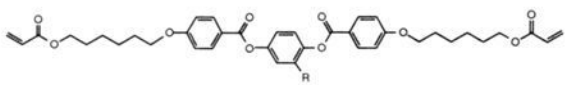

1 R=H (Crystal 108 Smectic (88) Nematic 155 Isotropic)

2 R=CH_3 (Crystal 86 Nematic 116 Isotropic)

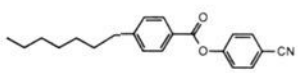

3 (Crystal 44 Nematic 56.5 Isotropic)

previous report by describing in more detail experiments with the methyl derivative **2**, mixed with a dielectric dopant, 4-cyanophenyl 4-heptylbenzoate[10] (**3**, 20%), added to provide the mixture with a strong response to electric fields.[11] While results with the two diacrylates are very similar, we have focused on **2** because of the lower and broader nematic temperature range it offers.[13] Detailed studies of the mesomorphic characteristics and photopolymerization processes of these monomers have appeared in the literature.[14] In this report, we also describe improved recording procedures, improved switching characteristics, photochemical fixing of the gratings, video microscopy of the dynamic gratings, and more detailed mechanistic models that describe the observed switching and fixing processes.

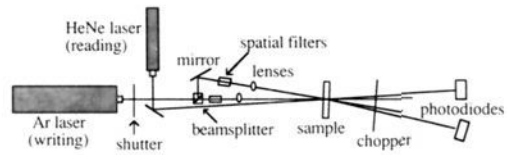

Figure 2. Two-wavelength phase-insensitive holography apparatus. Writing was achieved with blue light (488 nm), and reading was achieved with red light (633 nm).

Experimental Section

Materials and Sample Handling. Diacrylate **2** was provided by D. J. Broer. The photoinitiator H-NU 470 was a gift of Spectra Group Ltd., 1722 Indianwood Circle, Maumee, OH 43537.[15] The dielectric dopant 4-cyanophenyl 4-heptylbenzoate (**3**) was obtained from Aldrich. Batches of the monomer mixture, containing **2** with 20% **3** and 0.1% initiator (by weight), were prepared by dissolution of the components in methylene chloride followed by evaporation of the solvent with stirring. Phase-transition temperatures of the mixture (C 76 N 103 I) measured with a Perkin-Elmer DSC-7 differential scanning calorimeter (DSC) were somewhat lower than those for pure **2**. Optical samples were prepared by capillary filling into 6 μm thermostated cells assembled from indium/tin oxide-coated glass plates (from Applied Films Laboratory). The plates were also spin-coated with polyimide (SPI-2000, MicroSci) and rubbed unidirectionally on velvet before cell assembly. The cell spacing was achieved by using 6-μm-diameter glass fibers from Merck and verified through interferometry. The empty cell was adjusted in the holder until two or fewer fringes were visible with reflected red light, indicating that the spacing was uniform to within 0.6 μm. The samples were weakly absorbing at 488 nm ($A = 0.030$) to maximize writing uniformity in the thickness dimension. Temperature readings from the thermostatic controller were calibrated so as to match the clearing point of the monomer mixture from the DSC (103 °C). An electric field (an amplified 1-kHz sine wave, voltage reported as root mean square) was applied to the sample through alligator clip connections to the cell plates. Initial homogeneous alignment of the samples was verified by using a polarizing microscope.

Holography. The optical apparatus used to obtain our results was a two-wavelength phase-insensitive holography apparatus,[16] represented in Figure 2. Holographic gratings were recorded with crossed beams (488 nm) from an air-cooled argon ion laser (ILT 5490 ASF, coherence length = 50 m). The beams were expanded to 10–18 mm by using spatial filters and lenses. An aperture in contact with the sample allowed only the centers of the writing beams to pass. For small interbeam angles ($2\theta < 20°$), a circular aperture of 2.4-mm diameter was used, and for larger angles, a rectangular (2 mm × 4 mm or 2 mm × 6 mm) aperture was used. Reading was accomplished by using the 633-nm beam from a HeNe laser (Uniphase 1125P), positioned at the Bragg angle. The first-order diffracted and transmitted beams were chopped at 210 Hz and detected with matched photodiode detectors, each connected to a lock-in amplifier (Stanford SR510). The lock-in amplifiers were interfaced with MS-DOS computers. A lens was sometimes used to focus the reading beam.

Video or still images of the gratings were recorded by mounting a video camera or a 35-mm camera on a polarizing microscope. After a grating spot was written and tested for switching behavior, the sample was placed under the microscope (equipped with a red filter, CS 2-60, to prevent further photolysis) and the grating was located. The image of the grating was recorded on videotape as it was switched.

Results

Diffraction Experiments. In order to allow continuous monitoring of holographic efficiency, separate wavelengths of coherent

(8) (a) Domash, L.; Schwartz, J.; Nelson, A.; Levin, P. In *Image Storage and Retrieval Systems*, Niblack, W., Jamberdino, A. A., Eds.; SPIE: Bellingham, WA, 1992; Proc. SPIE Vol. 1662, pp 211–217. (b) Domash, L. H. In *Photonics for Computers, Neural Networks, and Memories*; Miceli, W. J., Neff, J. A., Kowel, S., Eds.; SPIE: Bellingham, WA, 1993; Proc. SPIE Vol. 1773, pp 372–376.

(9) Leith, E. N.; Upatnieks, J. *J. Opt. Soc. Am.* **1963**, *53*, 1377–1381.

(10) Karamysheva, L. A.; Kovshev, E. I.; Barnik, M. I. *Mol. Cryst. Liq. Cryst.* **1976**, *37*, 29–34.

(11) The preliminary results of ref 1a were achieved without an added dielectric dopant. With later batches of **1**, we were unable to reproduce these results without added dopant, and we conclude that an impurity in the first batch must have served as a dopant. This conclusion is consistent with the small, negative dielectric anisotropy ($\Delta\epsilon = -1.6$, 100 °C, 100 kHz) measured for **1**.[12] A much stronger electric field (100 V) was used in the previous work than in the present report (3 V).

(12) Broer, D. J. Personal communication.

(13) The usable nematic range is larger than indicated by the transition temperatures, since crystallization is slow. See Results section.

(14) (a) Broer, D. J.; Boven, J.; Mol, G. N.; Challa, G. *Makromol. Chem.* **1989**, *190*, 2255–2268. (b) Broer, D. J.; Hikmet, R. A. M.; Challa, G. *Makromol. Chem.* **1989**, *190*, 3201–3215. (c) Hikmet, R. A. M. *J. Appl. Phys.* **1990**, *68*, 4406–4412. (d) Hikmet, R. A. M.; de Witz, C. *J. Appl. Phys.* **1991**, *70*, 1265–1269. (e) Broer, D. J.; Mol, G. N. *Polym. Eng. Sci.* **1991**, *31*, 625–631. (f) Hikmet, R. A. M.; Lub, J.; Maassen vd Brink, P. *Macromolecules* **1992**, *25*, 4194–4199. (g) Hikmet, R. A. M.; Zwerver, B. H.; Broer, D. J. *Polymer* **1992**, *33*, 89–95. (h) Heynderickx, I.; Broer, D. J.; Van Den Boom, H.; Teesselink, W. J. D. *J. Polym. Sci., Part B* **1992**, *30*, 215–220.

(15) Shi, J.; Zhang, X.; Neckers, D. C. *J. Org. Chem.* **1992**, *57*, 4418–4421. H-NU 470 is referred to as DIMF in this paper.

(16) Pinsl, J.; Gehrtz, M.; Reggel, A.; Bräuchle, C. *J. Am. Chem. Soc.* **1987**, *109*, 6479–6486.

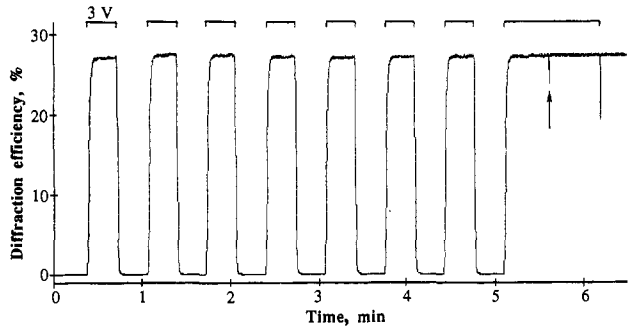

Figure 3. On/off diffraction switching of a grating written at 84 °C with an exposure of 9 s (3.2 mW/cm²) in the absence of electric field. Switching to the "on" state was accomplished by applying an ac field of 3 V. The interbeam angle was 2.6°, and the grating spacing was 10.8 μm. The observed modulation ratio was 650. Fixing of the grating in the switched state was achieved through a single-beam irradiation of 25 s while reading was paused at the arrow. A lens was used to focus the reading beam.

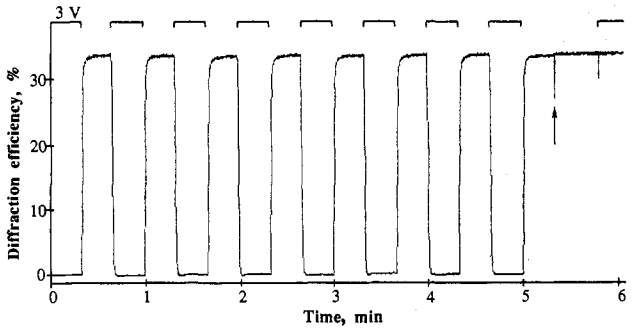

Figure 4. On/off switching of a grating written as in Figure 3, except that a 3-V electric field was applied during the writing step. Switching to the "on" state was accomplished by switching off the field. The observed modulation ratio was 200. A 15-s, single-beam exposure was used to fix the grating while reading was paused at the arrow. A lens was used to focus the reading beam.

light were used for the writing and reading processes. The 633-nm reading beam was not absorbed by the samples, nor did it interfere with the writing process. In general, writing and fixing were accomplished with short exposures (1–10 s) with two beams and one beam, respectively, of 488-nm light. Diffraction efficiency (η) refers to the ratio of the intensity of the diffracted beam to the intensity of the transmitted beam, the latter measured before the recording step. Most of our experiments were done in the thin-grating regime, where several orders of diffraction (from ±5 to ±14) were observed. Unless otherwise specified, diffraction results refer to first-order diffraction.

The results from a typical diffraction experiment are shown in Figure 3. After a 9-s writing exposure (not shown), weak diffraction was observed. A rapid 650-fold increase in diffraction, to 27%, was observed upon application of an alternating electric field (3 V), and the efficiency returned to the original value upon removal of the field. Subsequent switching cycles were nearly identical. Fixing of the high-efficiency hologram was accomplished with a single-beam irradiation of 25 s, after which the diffraction efficiency was unaffected by further changes in the applied field.[17]

Analogous experiments were done by writing gratings in the presence of nonzero fields. Figure 4 shows the changes in diffraction efficiency through writing at 3 V, switching repeatedly to 0 V, and then fixing at 0 V with a 15-s, single-beam exposure. Gratings written at intermediate fields (such as 3 V) could be switched by either increasing or decreasing the applied voltage. The diffraction characteristics obtained with this method were comparable to those obtained by writing at 0 V.

(17) Much shorter fixing irradiations were used, depending on sample age (see Results). This sample was 4-days old.

Aside from electric fields, temperature and pressure changes also allowed reversible modulation of diffraction efficiency after the writing step. Upon heating, small changes were observed until the nematic-to-isotropic clearing point was reached, when the efficiency rose markedly. Whether the maximum efficiency was more or less than that attainable with electric fields depended on the recording parameters (see below). Heating to 10–20 °C above the clearing point reduced the efficiency again to nearly zero. Recooling to below the clearing point restored the gratings to their original state, undamaged for further electrical switching operations. Pressure effects were not systematically investigated, but modulation of diffraction efficiency was observed when pressure was applied to the glass near the laser spot.

Many experimental parameters were varied in the diffraction experiments, and we found that the results depended strongly on these variables, and in many cases, the variables were closely coupled to each other. Included in our studies were variations in writing exposure (both time and intensity), interbeam angle, electric field strength, and temperature. We have not attempted to completely map the parameter space, a task made even more daunting when one considers that several characteristics of the diffraction are important, including efficiency, modulation ratio, switching speed, and switching durability. Rather, we have attempted to identify the general effect of changes in each parameter, both on the diffracted signal and on the other variables.

Exposure. Before exposure dependence of the diffracted signals could be analyzed, some issues relating to exposure had to be addressed. First, microscopic images of the gratings (see text below and Figure 5) showed a strong radial variation within each laser spot. Many of the spots had fixed centers, while the surrounding concentric regions showed varying degrees of switching. These patterns, clearly arising from the Gaussian intensity profile of the laser beams, signaled that the observed diffraction efficiencies were actually averages representing a significant range of exposures.[18] In addition to this inhomogeneity, a dependence of the switched signal on irradiation interval was also observed (i.e., a 3-s exposure was not equivalent to three 1-s exposures). Quantitative interpretation of sensitometric data for the switching media without accounting for these effects would be problematic.

The inhomogeneity within the laser spots was minimized by using a more square beam profile, obtained by expanding and collimating the Gaussian beams and passing only the centers through an aperture in contact with the front plate of the sample. In this way, the center ($^1/_8$–$^1/_4$ of the diameter) of the Gaussian profile was used for writing. This resulted in much more homogeneous spots, as observed by microscopy (Figure 6). Therefore, in order to minimize inaccuracies due to exposure inhomogeneity, we report herein only data that were obtained with this method.

Another complication concerning exposure was an observed dependence on the writing time interval and on the time between intervals. For a given overall writing time, more extensive writing was obtained through the use of longer or more closely spaced intervals. This effect was consistent with the observation of an induction period for each irradiation. When the intervals followed one another with short delays, the induction period was reduced in the succeeding intervals. Thus, with well-spaced intervals shorter than the induction period, little writing was observed, even after many intervals. Beyond this effect, the expected reciprocal relationship between intensity and time (exposure = intensity × time)[19] was reasonably well-established, at least for intensities between 0.3 and 6.0 mW/cm² (sum of the two beams).

Exposure inaccuracies were thus minimized by using expanded

(18) This effect has been used to advantage: Leclere, P.; Renotte, Y.; Lion, Y. *Appl. Opt.* **1992**, *31*, 4725–4733.

(19) Dainty, J. C.; Shaw, R. *Image Science*; Academic: New York, 1974; p 46.

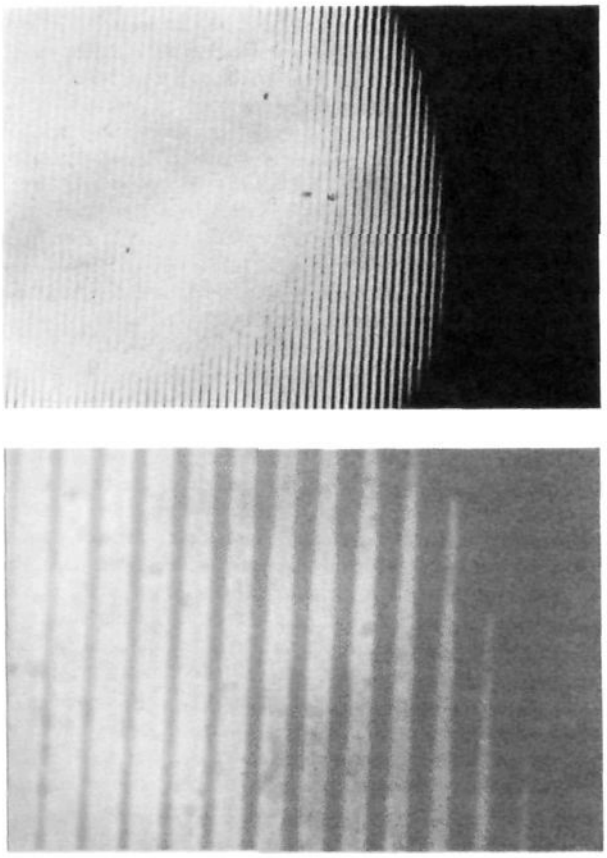

Figure 5. Images of a grating written under 4 V with Gaussian beams and switched to 0 V, as magnified by a microscope. The bottom image is an edge region magnified five times with respect to the upper image. The grating spacing was 10.8 μm. A strong variation in the width of the grating lines is apparent, with the permanent regions appearing narrow at the edge and wide toward the center. A large region in the center of this spot was fixed.

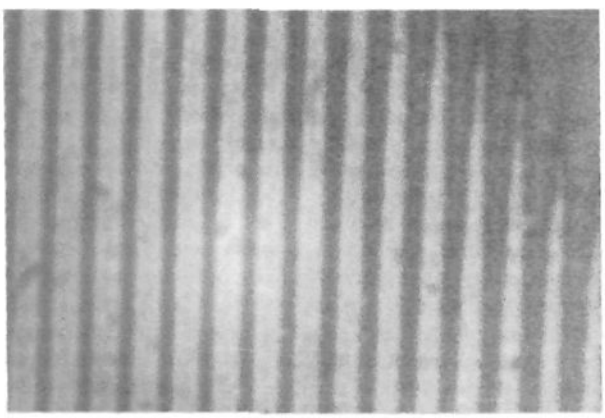

Figure 6. Edge of a grating written under 4 V with expanded and clipped (square) beams and switched to 0 V, as magnified by a microscope. The grating spacing was 10.8 μm. The width variation is still apparent in this area near the edge but is much less severe than in Figure 5. All regions of this spot were switchable.

and clipped beams for writing and by using evenly and closely spaced irradiation intervals. Sample data showing the dependence of diffraction efficiency, in both switched and unswitched ("on" and "off") states, on the exposure time are shown in Figure 7. Qualitatively, one may conclude that the unswitched films are reasonably typical in their recording characteristics, while strong, sharply varying nonlinearities are observed in the switched state. The high sensitivity of the switched signal to exposure is clearly the reason that the inhomogeneity and interval effects were so

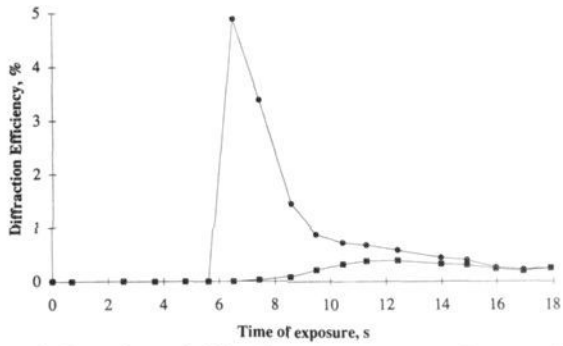

Figure 7. Dependence of diffraction efficiency on time of exposure for a grating written with expanded and clipped beams in the absence of field. Efficiency in the switched state (3 V) is represented by circles, and efficiency in the unswitched state (0 V) is represented by squares. The writing intensity was 3.2 mW/cm².

Table 1. Dependence of Diffraction Switching Characteristics upon Interbeam Angle

2θ (deg)	Λ (μm)	maximum η (%)[a]	optimum E (V)[b]	η at 104 °C
2.6	10.8	21[c]	3	9
7.5	3.7	9	10	
19.2	1.5	4	20	
45.0	0.64	1	29	6
90.0	0.35	0.2	≥50	

[a] In the switched state with applied field. [b] Optimum electric field for low exposures. [c] With a focused reading beam, values up to 34% have been measured for 2θ = 2.6°.

readily apparent. The maximum efficiency reached in the unswitched state was found to depend significantly on recording parameters.

In some experiments, inhomogeneities were further reduced through focusing of the reading beam onto a smaller region of the written spot. Even with the flatter exposure profile obtained with the clipped beams, inhomogeneities were sometimes observed due to interference effects arising from variations in substrate thickness. The thickness variation of the cell spacing was small (<0.6 μm over the 12-mm window), and the observed interference fringes were primarily due to the substrates. The effect of this interference on the writing process was amplified by the sharp and delayed sensitivity (Figure 7).

The sensitivity to the writing beams was found to depend significantly upon the age of the samples. Samples kept for a week to 10 days at 84 °C allowed recording and switching of gratings almost identically to fresh samples, except that longer exposures were required. The longer exposures were due to longer induction periods, suggesting that prolonged heating caused either decomposition of the initiator or production of an inhibitor. After 10 days or so, the samples began to significantly scatter light.

Figure 7 suggests that fixing might be accomplished as conveniently with two beams as with one, since a reasonably short exposure is required to eliminate the switching response. Indeed, a two-beam exposure in the switched state was found to the fix the gratings.

Interbeam Angle. As one varies the interbeam angle, the grating spacing also changes, as described by Bragg's law (eq 1, where

$$\lambda = 2\Lambda \sin \theta \qquad (1)$$

λ is the wavelength of light, Λ is the grating spacing, and 2θ is the interbeam angle outside of the film).[20] While most of our experiments were done with small angles (large spacings), some results were obtained with large angles. Table 1 shows that the electrical switching process became less favorable as the grating spacing decreased: the required electric field increased, while

(20) Tomlinson, W. J.; Chandross, E. A. *Adv. Photochem.* **1980**, *12*, 201–281.

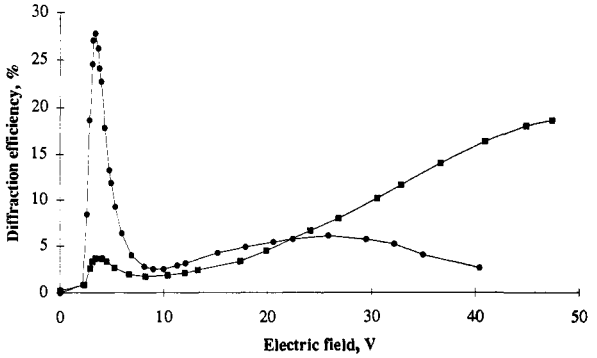

Figure 8. Dependence of diffraction efficiency on applied field strength for a grating written in the absence of field with exposures of 16 s (circles) and 44 s (squares). The writing intensity was 3.2 mW/cm².

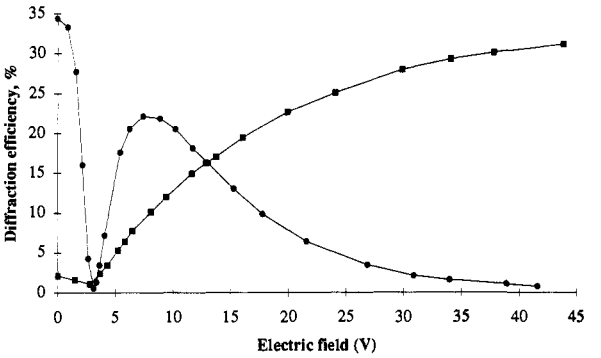

Figure 9. Dependence of diffraction efficiency on applied field strength for a grating written under a field of 3 V with exposures of 14 s (circles) and 35 s (squares). The writing intensity was 3.2 mW/cm².

the attainable diffraction efficiency decreased. However, the response of the diffraction to heating the sample above the clearing point did not decrease as significantly. Another effect observed for the smallest grating spacings was that attempts to fix the holograms were often unsuccessful, resulting instead in decreased efficiency.

Electric Field. The diffracted intensity, even in the switched state, was highly dependent upon the applied electric field, and this dependence was strongly affected by changes in exposure, interbeam angle (Table 1), and applied field in the writing step. Figure 8 shows the field dependence for gratings written with two different exposures in the absence of applied field, and Figure 9 shows the analogous dependence for gratings written under a field of 3 V. Electric field also had a large effect upon switching time, with faster switching occurring upon application of higher fields, as expected.[21]

Temperature. Temperature had a primary effect on the diffraction experiments through the phase behavior of the samples. Even though the monomer mixture has a melting point to the nematic phase of 76 °C, recrystallization is slow, requiring several hours at 44 °C and 10–20 min at room temperature. The usable nematic range is thus much larger than the 76–103 °C range implied by the transition temperatures. Most of our experiments were conducted at either 84 or 44 °C, but writing and switching was successfully performed from room temperature to 100 °C. Unless otherwise noted, the temperature was 84 °C.

The dependence of efficiency on temperature was minor within the nematic range. Slightly higher switched efficiencies were obtained when a grating was written at 84 °C and then cooled to 44 °C. Temperature did have a significant effect upon switching times, with shorter times for both application and removal of the electric field observed at higher temperature.

Summary of Switching Properties. Three properties that relate to the switching of the gratings are the on–off ratio of diffraction efficiencies, switching time, and switching durability. When the exposure was near optimum, very high modulation ratios were observed, typically 100–500, but values as high as 8000 have been measured. Switching times at 84 °C were about 2 s after application of the field (3 V) and about 1 s after removal of the field. Shorter times were observed after application of higher fields, for example, less than 0.033–0.3 s for 16 V. Switching durability was also very good, with minimal (6%) degradation in modulation ratio observed after 10^5 cycles (5 days, 0.25 Hz).

(21) Meier, G.; Sackmann, E.; Grabmaier, J. G. *Applications of Liquid Crystals*; Springer-Verlag: New York, 1975; p 13.

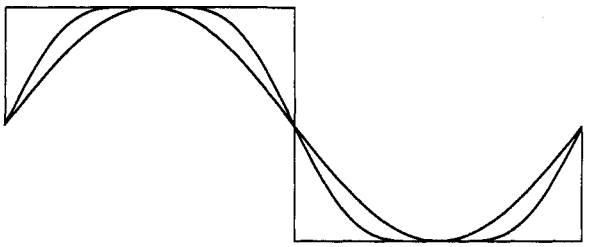

Figure 10. Shapes of the three refractive index profiles used for the simulation of diffracted intensities: sine wave, square wave, and, between them, the optimized form of sin x + δ sin $3x$, with δ = 0.13.

Video Microscopy. Direct observations of the gratings were made by optical microscopy,[22] and dynamic images of the gratings being switched were recorded on videotape. These observations proved immensely valuable in the evaluation of recording and switching mechanisms, as well as in the design of improved recording procedures.

The image of a grating in the switched state, between crossed polarizers (with the alignment direction at 45° to the polarizer axes), is shown in Figure 6. In the unswitched state, the grating was barely perceptible, if at all, and the entire sample was bright. In the switched state, high contrast was observed between the polymeric and monomeric regions of the grating. Sharp boundaries between regions made the switched gratings appear more nearly binary (square) than sinusoidal, although these details of the images should be interpreted cautiously.[23] These images allowed direct measurement of the grating spacing, which agreed with the expected values from Bragg's law (eq 1). A frame-by-frame analysis of the videotape also allowed measurements of the switching times. Good agreement was observed between switching times obtained from the video and from the diffraction experiments. If the switching event was complete within a single frame, an upper bound of 0.033 s was indicated for the switching time.

One of the first and most important observations made with the microscope was the inhomogeneity of the Gaussian laser spots (see above). Figure 5 shows the image of such a laser spot in the switched state. The center of the spot was unresponsive to the electric field, while the region surrounding it showed high-contrast switching. Also apparent in these images is a radial variation in the width of the fringes. The grating spacing remained constant, but the monomeric (alignable) regions were wider with respect to the polymeric (permanent) regions toward the perimeter of the spot.

For comparison to Figure 5, Figure 6 shows a similar grating recorded using the square-beam method. Spots recorded in this way were generally fully switchable, with little apparent width variation except near the edge of the spot.

Another important observation made with the microscope was that the relative widths of the permanent and alignable regions were field dependent. As the applied field was increased, the alignable regions were observed to widen as the "permanent" regions narrowed. At the same time the diameter of the spot was slightly reduced as the narrowest parts of the permanent regions, at the edge of the spot, were eroded entirely.

(22) Others have used microscopy to study gratings, and sophisticated analytical techniques have been reported: Rupp, R. A. *Appl. Phys. B* **1986**, *41*, 153–168.

(23) Rupp, R. A.; Krätzig, E. *Phys. Status Solidi A* **1982**, *72*, K5-K8.

Table 2. Experimental and Simulated Efficiencies for Various Diffraction Orders[a]

order	experimental[b]	sine wave[c]	square wave[d]	$\sin x + 0.13 \sin 3x$[e]
0	4.1	4.1	4.1	4.1
1	33.7	30.5	35.6	34.1
2	6.4	11.7	0	6.4
3	2.6	1.6	4.0	2.1
4	0.79	0.11	0	1.0
5	0.31	0.005	1.4	0.18
6	0.10	0.000	0	0.031
7	0.038	0.000	0.73	0.007
8	0.013	0.000	0	0.001

[a] Efficiencies are listed as percentages. Efficiencies of the negative orders are identical to those of the positive orders in the simulations and within experimental error for the experimental data. Simulated values have been reduced by 8% to match the light losses in the experimental data. These losses are primarily due to backward diffraction. [b] For a grating written under 3 V and switched to 0 V at 84 °C ($2\theta = 2.1°$). [c] Peak-to-peak amplitude = $\Delta n = 0.068$. [d] Peak-to-peak amplitude = $\Delta n = 0.046$. [e] Peak-to-peak amplitude = $\Delta n = 0.058$.

As shown in Figure 9, when a grating was written under an intermediate field, diffraction efficiency could be increased by either increasing or decreasing the field strength. Such gratings appeared under the microscope as one would expect, with high contrast at zero and high fields and with no contrast at the same field used in the writing step.

Simulation of Diffraction Efficiencies. We have attempted to fit the measured intensities of the various diffraction orders from the thin-regime gratings ($\Lambda = 10.8\ \mu$m) to values calculated under the assumption of a grating profile.[24] Three profiles were used (Figure 10): sine wave, square wave, and a two-term Fourier series ($\sin x + \delta \sin 3x$). The last profile, for δ values between zero and about 0.15, is between the sine and square functions, with broader peaks and steeper slopes than a sine wave.

Calculated intensities for the three profiles are listed with a representative experimental data set in Table 2. The sine and square profiles clearly provide unsatisfactory fits to the data, while the optimized intermediate profile ($\delta = 0.13$) provides a much closer correlation.[25] The results show that these gratings are well within the thin-grating regime.[26]

Discussion

All of the results presented above are consistent with the recording/switching mechanism shown in Figure 11. The monomer mixture, aligned by the rubbed surface into a monodomain with vertical, homogeneous (parallel to the substrates) orientation, is photopolymerized by the crossed writing beams. This leads to a grating composed of cross-linked polymer in the regions of constructive interference and monomer in the regions of destructive interference. The refractive index modulation, Δn, in this unswitched state is very small and primarily attributable to the difference in concentration of the acrylate functionality. Upon application of an electric field, only the monomeric regions are nonviscous enough to realign to the homeotropic orientation (perpendicular to the substrates), producing a very large Δn in this switched state due to the birefringence (refractive index anisotropy) of the liquid crystal. If the electric field is removed, the monomer regions relax to their previous surface-induced orientation, and the hologram is again in the unswitched state. On the other hand, if the sample is irradiated with a single writing beam while the field is on, the switched state can be made permanent, even in the absence of the field.

(24) (a) Magnusson, R.; Gaylord, T. K. *Opt. Commun.* **1978**, *25*, 129–132. (b) Magnusson, R.; Gaylord, T. K. *J. Opt. Soc. Am.* **1978**, *68*, 806–809.

(25) The use of higher order Fourier series provides even better fits to the data, especially in the higher orders. Sponsler, M. B. *J. Phys. Chem.*, submitted for publication.

(26) Magnusson, R.; Gaylord, T. K. *J. Opt. Soc. Am.* **1978**, *68*, 809–814.

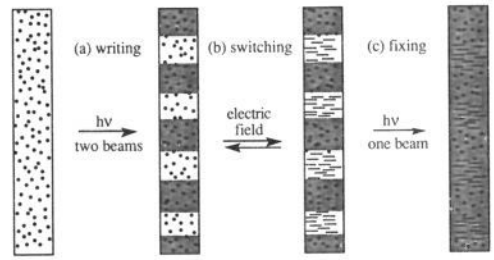

Figure 11. Mechanistic model for the (a) writing, (b) switching, and (c) fixing processes in the liquid crystalline monomer samples. A portion of the top edge of the sample is depicted as viewed from above. Initially, the molecular alignment is vertical and homogeneous, as determined by the substrate rubbing direction. During the holographic writing process, photopolymer (shading) is formed in the regions of constructive interference. Under the influence of an electric field, the monomeric regions are reversibly realigned to the homeotropic orientation. Further irradiation with a single laser beam causes fixing through polymerization of the entire grating.

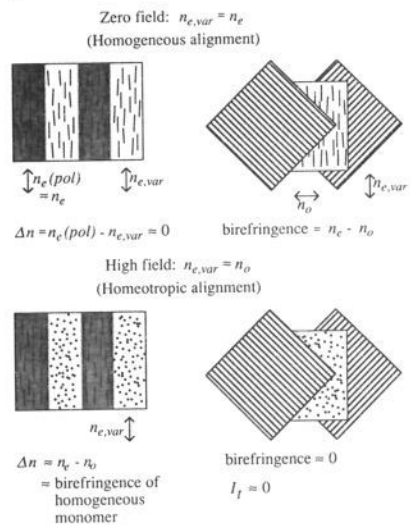

Figure 12. Relationship between anisotropic refractive indices and the important refractive index differences for our diffraction experiments (left) and birefringence measurements with crossed polarizers (right). Variables: n_e and n_o are the extraordinary and ordinary refractive indices of the monomer, $n_{e,var}$ is the variable refractive index that depends on the applied field, and $n_e(pol)$ is the extraordinary refractive index of the polymer. A face of the sample is depicted as viewed along the normal.

The simple model outlined above, the same one used to explain our preliminary diffraction results,[1a] is strongly supported by all of our diffraction and microscopy experiments. When viewed between crossed polarizers under the microscope (Figure 5 and 6), gratings written at 3 or 4 V have lines that remain bright in both unswitched and switched states (polymer) interlaced with lines that become dark in the switched state (monomer). The dependence of the diffraction characteristics (efficiency, modulation ratio, and switching speed) on the various experimental parameters (exposure, interbeam angle, field strength, and temperature) is fully consistent with the proposed mechanism. This data has further allowed us to refine the model by inclusion of several details concerning the monomer/polymer boundaries.

When viewed with the microscope, the visual change in the grating upon switching is striking, going from almost imperceptible to high contrast. The birefringence differences between regions that control the contrast in these images observed through the polarizing microscope are directly related to the refractive index differences that control diffraction (Figure 12). Thus, the sharp on/off visual effect is mirrored in the diffraction efficiency modulation, which was measured often in the 100–500 range but was sometimes over 1000. With numbers in this range, the ratio

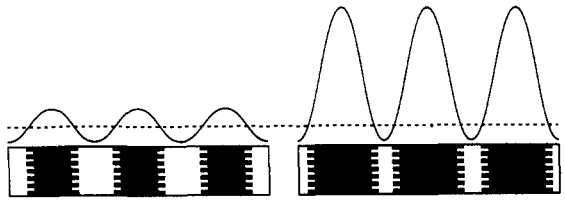

Figure 13. Exposure threshold model for writing of gratings. The dashed line is the exposure threshold, the solid line is the sinusoidal exposure profile, and the resulting gratings are represented below, with the permanent regions shaded, the alignable regions unshaded, and the boundary regions dashed. On the left, exposure is at the optimum for strong diffraction in the switched state, and on the right, the exposure is four times greater.

is much more dependent on the off-state diffraction (denominator), and such large numbers are possible only because the on-state diffraction increases so sharply at low exposure, where the off-state diffraction is still small.

Exposure Dependence. The exposure dependence of the diffraction in the switched and unswitched states (Figure 7) is very informative. In the unswitched state, the samples show an exposure dependence similar to that reported for many recording materials, with a reasonably linear region and a saturation region at high exposure. In contrast, the switched-state dependence is highly nonlinear, with a small exposure window that allows good switching. The greatest modulation is achieved with exposures that slightly exceed the exposure threshold, below which diffraction is not observed with or without the field. With increasing exposure, the modulation ratio decreases as the switched signal decreases and the unswitched signal grows, and ultimately the switching effect ceases.

The observed exposure dependence is explainable with the model in Figure 11 and by noting that the exposure profile is sinusoidal. We will presume that the exposure threshold, on a microscopic level, corresponds to the exposure necessary to produce polymer rigid enough to withstand the subsequent switching field. Figure 13 represents this threshold as a fixed horizontal line and the exposure profile as a sine wave whose amplitude is proportional to exposure (time and intensity). Using this model, we may expect that the maximum diffraction in the switched state would be achieved through an exposure approximately twice that of the threshold (plus the induction period), resulting in equally wide alignable and permanent regions. Increasing the exposure beyond this point will result in wider permanent regions and narrower alignable regions, with a corresponding decrease in on-state diffraction. Under prolonged exposure, the monomer regions will become too narrow to allow switching and will ultimately be converted completely to polymer.

The threshold model of Figure 13 will be used to explain many of our results, but before proceeding, we will attempt to further clarify it. Taken in its simplest form, this model would imply that, through photopolymerization and electric field switching of the sample, the sinusoidal exposure profile would produce a rectangular wave or binary grating, with sharp boundaries of orientation and refractive index occurring where the exposure profile crosses the threshold. A more realistic interpretation would allow for a finite boundary region, as shown in Figure 13. Indeed, our data are most consistent with a refractive index profile having a shape between that of a sine wave and that of a square wave (see Table 1). Note that for simplicity, the boundary region is not depicted in Figure 11.

A primary feature of the threshold model is the prediction of exposure-dependent widths for the alignable and permanent regions. This feature has been clearly observed by microscopy and is most obvious in gratings written with Gaussian beams (as delivered by the laser). In these gratings, a large width variation is apparent within the laser spot, with the widest alignable regions occurring at the perimeter and the widest permanent regions occurring at the center.

Electric Field Dependence. The observed field dependence, shown in Figure 8, is also explainable with the threshold model, if we make the added clarification that the threshold (*i.e.*, the height of the dashed line in Figure 13) is dependent on the field. This is to be expected, since regions of lightly cross-linked polymer would likely resist small but not large fields. Thus, higher fields should lead to wider alignable regions, and this, in fact, has been observed under the microscope. At low exposure, where the alignable regions are already wide, high fields are then less effective than low fields at producing strong diffraction. However, at higher exposure, where the alignable regions are narrower than the permanent regions, high fields are most effective.

As mentioned above, boundary regions were not included in Figure 11. In addition, the figure also idealizes the electric field reorientation of the alignable regions. In fact, the molecules nearest to the rubbed surface of the substrate remain parallel to the surface even at high fields.[27] The most readily aligned molecules are those in the center of the sample, and by increasing the voltage, one can align molecules closer and closer to the surfaces. A similar situation should exist with respect to the surfaces at the boundaries with the permanent regions. Thus, the apparent widening of the alignable regions with increasing field may be attributed partly to this effect. Also, as the alignable regions become narrower with higher exposures, higher fields are necessary in order to overcome these elastic forces at the boundaries with the permanent regions.

The sharp diffraction efficiency peak at 3 V for the low-exposure data in Figure 8 is explainable in terms of overmodulation of the refractive index. In transmission holograms, diffraction efficiency shows oscillations with increasing Δn, although many recording materials are incapable of reaching the first maximum. For thick gratings, in which the sample thickness is large relative to the grating spacing, the efficiency oscillates between 0 and 100%, whereas for thin gratings, the first maximum is 33.9% for a sinusoidal modulation.[20] The maximum value is higher by a few percent for gratings that have sharper boundaries but can also be lower if the two regions have different widths. In Figure 8, the maximum at 3 V is 28%, while in Figure 9 and in other experiments maxima as high as 34% have been observed.[28] The second, broader maximum in Figure 8, at about 25 V, may indicate that, for this particular grating, equal widths for the alignable and permanent regions are obtained at this voltage. The high-exposure data also show a peak at 3 V, with its small size attributable to a large width discrepancy.

The explanation of overmodulation for the sharp decrease beyond 3 V is well-supported by other data besides the value of the peak efficiency. First, the intensities of all of the diffracted orders at 3 V match very well the simulated values for the optimum modulation condition. From this simulation, we can extract a value for Δn of 0.058. An independent measurement of Δn was obtained by measuring the transmitted beam intensity (I_t) as a function of field when the sample is placed between crossed polarizers (with the liquid crystal alignment direction at 45° to each polarizer, Figure 12). Under high field (>15 V), the sample is nonbirefringent and $I_t \approx 0$. When the voltage is decreased, a maximum in the intensity is observed at 3 V. Using the standard equation that describes the electric field alignment of nematic phases (eq 2),[29] the birefringence ($n_{e,var} - n_o$) at 3 V was calculated

$$I_t = I_0 \sin^2(\pi d(n_{e,var} - n_o)/\lambda) \quad (2)$$

(27) deJeu, W. H. *Physical Properties of Liquid Crystalline Materials*; Gordon and Breach: New York, 1980; p 21.

(28) As noted in Table 2, the experimental values are low by about 10%, due to light losses to backward diffraction.

(29) Kelker, H.; Hatz, R. *Handbook of Liquid Crystals*; Verlag: Deerfield Beach, FL, 1980; p 189.

to be 0.053, and the birefringence at 0 V was found to be 0.114. (This value is close to the literature value of 0.13 for pure **2** at 84 °C at 589 nm.[14b,f]) In eq 2, I_0 is the incident intensity (corrected for reflection losses), d is the sample thickness (6 μm), $n_{e,var}$ is the extraordinary refractive index that depends on field strength, and n_o is the ordinary refractive index. Assuming that $n_{e,var}$ has the same field dependence in the presence and absence of a grating, we can then deduce that Δn in a grating written at 0 V and switched to 3 V should be $0.114 - 0.053 = 0.061$, in good agreement with the value obtained by simulation. Further evidence was obtained by using thicker cells (10–18 μm), in which case multiple diffraction efficiency maxima were observed as the field was varied, as expected.

The complication of overmodulation is removed in the data for gratings written at 3 V (Figure 9). In this case, the grating can be switched either by increasing or decreasing the field, and the sign of Δn is opposite for these cases. However, the birefringence of the liquid crystal is not large enough to allow overmodulation in either direction. Thus, the data of Figure 9 can be explained with the exposure-dependent width effect. In this case, the driving force in the switching to lower fields is the same rubbed-surface effect that is used to align the sample initially. Clearly, these forces are not strong enough to provide strong switching after extensive exposure. These forces must compete with similar surface forces, arising from the boundaries of the alignable and permanent regions, that tend to keep the alignable regions aligned with the permanent regions. As the alignable regions become narrower with exposure, the contact area with the rubbed substrate decreases and the interactions at the boundary surfaces dominate.

Interbeam Angle Dependence. Very similar arguments suffice to explain the effects of increasing the interbeam angle (Table 1), which causes the grating spacing to decrease. Smaller spacing means narrower alignable regions, so the fact that larger fields were required for optimum switching is in line with the exposure-dependent field effects noted above. As the spacing decreased, the observed diffraction efficiency also decreased, probably indicating that the boundary regions played an increasingly dominant role. Some of the phenomena that lead to finite boundary regions are not affected strongly by the change in exposure profile. These include movement of initiating species away from the point of absorption through polymer growth and diffusion, and boundary surface control over liquid crystal orientation. Thus, the boundary regions should become more significant as the permanent and alignable regions narrow.

Temperature-Induced Switching. In the developing (switching) process, an alternative to electric field-induced modulation of orientation is the temperature-induced modulation of liquid crystalline order. As the gratings were heated to above the clearing point of the monomer mixture (103 °C), diffraction increased. The diffraction efficiency was much less sensitive to grating spacing than with electric field switching. This can be explained by noting that the boundary surfaces can have little effect upon the isotropic phase, while their effect on nematic orientation is quite significant. Thus, the boundary regions should be narrower for the heated gratings, preventing them from dominating even with a small spacing. Additional evidence for narrower boundary regions comes from the intensity pattern of the various diffracted orders. While the field-switched gratings showed a monotonically decreasing intensity pattern, the heated gratings showed a visible extinction of some orders (either orders 2 and 4, or 3). This is indicative of a significant sharpening of the Δn boundaries.[30]

When the gratings were heated to over 120 °C, the diffraction efficiency decreased, giving almost no diffraction above 140 °C. By recooling the samples, the changes were shown to be reversible. This apparently indicates that the "permanent" regions were converted also to an isotropic phase at these temperatures, in apparent contrast to the report stating that the polymer from **1** remains birefringent even to 300 °C.[14a] The discrepancy is explained by the fact that the polymeric regions of our gratings are much less extensively cross-linked than a fully polymerized sample. Indeed, when additional fixing irradiation was done, beyond that necessary to prevent the electric field response, the grating became fixed with respect to heating as well. An interesting phenomenon was observed when a fixed, weakly diffracting ($\eta = 3\%$) grating was heated: the diffraction efficiency increased to 30% at 120 °C and then decreased gradually to 15% at 140 °C, and the changes were reversible upon cooling. This observation correlates well with the observation, from microscopy, that the permanent regions become narrower as the temperature is increased.

Characteristics of the Photopolymerization. Extensive data exists concerning the photopolymerization of diacrylates **1** and **2**,[14] and this information serves to further clarify the grating structure. In one literature study,[14g] the shrinkage properties of the diacrylate monomers during polymerization were investigated. Overall, shrinkage was found to be low, 4–7% for **2**, relative to that for typical acrylates, 11–15%. This effect, attributed to tight packing of the monomer, should lead to a less pronounced density grating, minimizing the off-state diffraction. Furthermore, shrinkage was found to be anisotropic, with the principal component occurring along the direction of alignment. In our experiments, this corresponds to the direction parallel to the grating lines. This should further reduce the contribution of monomer diffusion to Δn in the recording process, since shrinkage occurs primarily within each fringe and not across fringes.

This anisotropic shrinkage effect is probably responsible for the decrease in diffraction efficiency that we encountered while attempting to fix the low-period gratings. In the fixing stage, polymerization occurs simultaneously in the two regions of the grating. However, the polymerization rate is known to be highly dependent upon the percent conversion,[14a] which is different in the two regions. Therefore, uneven shrinkage presumably causes stress that builds up as the sample loses its fluidity. Apparently, the wider fringes studied can withstand this stress, while the finer fringes undergo distortion. This effect was not observed under the microscope, because the finest grating lines were not visible with our microscope. The observation limit was about 1.5 μm.

In the first report concerning **2**,[14b] refractive index changes during polymerization were presented. These data show that when **2** is polymerized at lower temperatures, almost no change in n_e is detected, while n_o increases by about 0.03. Given the shrinkage properties discussed above, this suggests that factors other than density are important in determining the index changes.[14b] In any case, the fact that n_e remains nearly constant (presumably also in our doped samples) fortuitously leads to very small Δn in the absence of switching.

The notion, discussed above, that the polymer–monomer boundaries are sharper than the exposure intensity gradient is well-supported by the reported polymerization kinetics of **1** and **2**.[14a,b] The rate of polymerization was shown to increase abruptly to a maximum at about 20% conversion and then decrease. Both the induction period and the rapid acceleration should serve to sharpen the monomer–polymer boundaries relative to the sinusoidal intensity gradient, since a relatively small exposure increment will be responsible for a large portion of the conversion from monomer to polymer. This is the case at least up to conversions of 50%, judging from the published kinetics for **1**, at which point the polymerized regions are probably permanent even at the highest fields used in our study. Given the high cross-link density provided by the difunctional monomers, relatively low conversion to polymer is required to prevent electric field switching. This is apparent from the heating experiments with fixed gratings, described above.

The rapid acceleration reported in the polymerization of the

(30) Diffraction from a square-wave grating results in complete extinction of the even orders, excluding the zeroth order.[24b]

difunctional monomers may have another important effect on grating formation. This acceleration, known as the Trommsdorff effect, is attributed to a decrease in the termination rate, caused by a progressive loss of diffusional mobility of the propagating radicals.[14a] As the termination rate decreases, the chain lengths increase, meaning that polymer growth can occur farther from the point of initiation. This effect, combined with the intuitive expectation that polymer growth should occur primarily in the direction perpendicular to the molecular axes,[14a] presumably leads to an increased rate of polymerization into and through the alignable regions. These considerations probably contribute significantly to the sharp rise and fall of the switched signal with respect to exposure (Figure 7).

The observation of a significant induction period in our experiments is best explained by the presence of oxygen, which acted as an inhibitor.[3] During irradiation, polymerization did not begin until oxygen was depleted. If irradiation was stopped and then restarted, another induction period was observed if sufficient time had passed to allow diffusion of oxygen from surrounding regions or from the destructive interference regions. One sample was prepared under nitrogen in order to test this explanation, but the sample polymerized under the dim light conditions required for capillary filling. This experiment lends indirect support to the explanation. The presence of an inhibitor thus eases sample handling, and it may have another practical benefit. Traces of oxygen that remain when polymerization begins may serve to slightly delay the Trommsdorff effect and the growth of polymer into the alignable regions.

A modified explanation for the writing and switching processes might be suggested by a report of hologram writing in mixtures of nonreactive liquid crystals with isotropic monomers.[7c] In these materials, polymer-dispersed liquid crystals (PDLCs) are formed through phase separation as the monomer is polymerized, providing switchable holograms. Our experiments do not rule out the possibility that some phase separation of **3** occurs, but this process cannot explain our results without the mechanism of Figure 11. For example, the low fields required for switching in our samples are uncharacteristic of PDLC materials with small domains. Furthermore, the fact that our samples are fixable argues against extensive phase separation.

Conclusions

Dynamic gratings with spacings from 10.8 to 0.35 μm were prepared by photopolymerization of a liquid crystalline monomer sample with interfering laser beams. The gratings were composed of alternate regions that are polymeric and monomeric, or permanent and alignable. The alignable regions were reversibly manipulated with respect to orientation by application of an electric field or with respect to order by heating. The changes that occurred during these switching events were monitored through the diffraction properties of the gratings. These experiments provided details about the structure of the gratings, including the boundaries separating the permanent and alignable regions. In addition, these experiments demonstrated the potential utility of such materials as switchable holographic recording media. Images of the gratings obtained through optical microscopy supported the conclusions about grating structure and provided valuable information about homogeneity of the irradiated spots.

Our results show that holographic experiments can provide valuable information about photopolymerization reactions in liquid crystals, especially when coupled with direct observation of the gratings. For example, kinetic data are obtainable directly, along with information about the development of polymer rigidity with respect to the aligning forces of applied fields and the randomizing effects of temperature. Through variations of exposure, field strength, and interbeam angle, information concerning the polymer–monomer boundaries can be obtained, which bears directly on issues such as anisotropic growth distances of the polymer chains. In this report, several conclusions were facilitated or corroborated by careful and detailed studies in the literature concerning the monomers and their polymerization processes; however, even in the absence of such data, diffraction experiments would provide meaningful data.

The gratings studied in this work offer a potentially useful architecture for the control of molecular orientation. The fringes are stacked layers, micron or submicron in size, with alternating molecular orientation.[31] They could be used to provide absolute and relative orientational control of solute molecules, either passively or actively, perhaps serving as organizational media for molecular electronic structures.[32] The gratings may be considered as two-dimensional polymeric structures with some similarity to the two-dimensional polymers of Stupp and co-workers.[33] Our materials have considerably thicker layers but offer the opportunity to modulate orientation.

Acknowledgment is made to the W. M. Keck Foundation and to the Camille and Henry Dreyfus Foundation New Faculty Award Program for partial support of this work.

(31) An alternative approach to such a structure is based on azobenzene photochemistry: Gibbons, W. M.; Shannon, P. J.; Sun, S.-T.; Swetlin, B. J. *Nature* **1991**, *351*, 49–50. Chen, A. G.; Brady, D. J. *Appl. Phys. Lett.* **1993**, *62*, 2920–2922.

(32) Bowden, M. J. In *Electronic and Photonic Applications of Polymers*; Bowden, M. J., Turner, S. R., Eds.; ACS Advances in Chemistry Series No. 218; American Chemical Society: Washington, DC, 1988; Chapter 1.

(33) Stupp, S. I.; Son. S.; Lin, H. C.; Li, L. S. *Science* **1993**, *259*, 59–63.